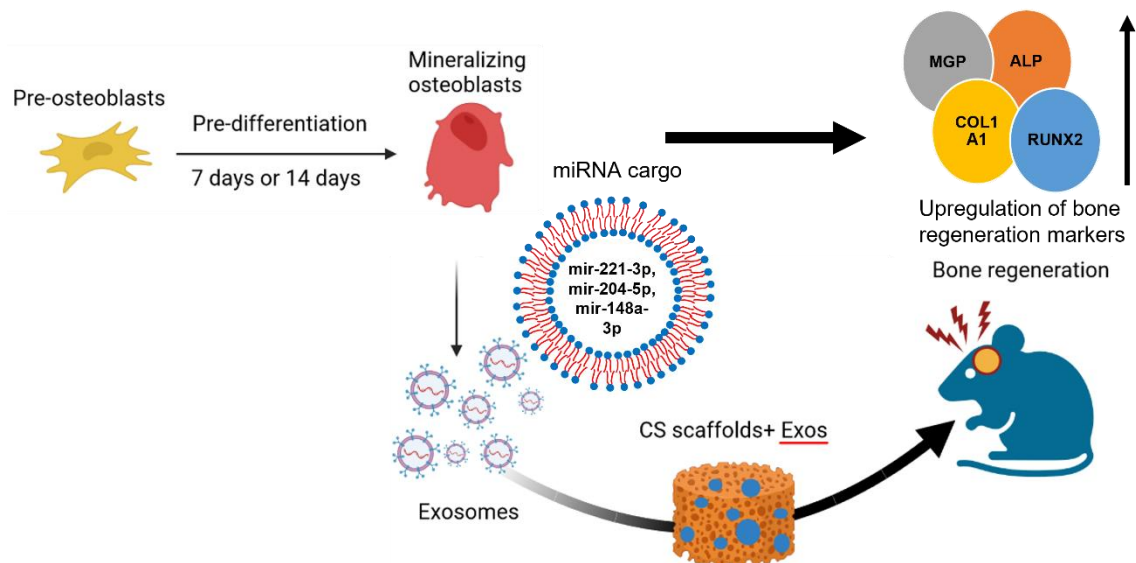# Mineralizing bone cell-derived exosomes integrated with polymeric scaffolds promote bone tissue regeneration by transferring their miRNA cargoes

Graphical representation: Potential role of mineralizing cell-derived exosomes and their small RNA (miRNA) cargos in enhancing the host bone cell mineralization *in vitro*. These exosomes integrated with covalently cross-linked chitosan scaffold have therapeutic applications and can be used for regeneration of critical size calvarial defects in rats.

1. Introduction

The treatment of bone fractures has been a clinical burden to individuals suffering with critical-size bone defects[1, 2]. Bone regeneration is a very complex, but well-orchestrated continuous remodelling process of bone formation. The entire adult life witness bone as a tissue which possesses a tremendous inherent capacity for regeneration through the coordinated activity of osteoclasts (OCs) and osteoblasts (OBs) [3, 4]. However, in case of large defects, where the injury goes beyond a critical limit, the bone will not be able to self-heal without surgical and therapeutic intervention[5, 6]. In case of a major bone fracture, a part of the bone is completely or partially broken causing pain and loss of functionality[7]. From a long period, these defects have been treated with autografts, allografts and xenografts, but some of the major limitations involved are immunological rejection, transplant failure, limited sources of donor, and disease transmission [8, 9]. Due to the notable limitations involved with the direct use of stem cells like uncontrolled proliferation, immune rejection, teratoma formation, the recent study has shifted its gear towards the use of cell-free therapy in bone regeneration [10, 11, 12, 13]. With the increasing focus on cell-free therapy, the role of exosomes in maintaining bone homeostasis has been extensively explored. Exosomes are nanovesicles (about 50-150 nm in diameter) that are secreted by most of the eukaryotic cells following an endosomal pathway[14, 15]. Exosomes contain several vital information in the form of miRNAs, mRNAs, proteins, and lipids protected inside their lipid bilayer structure[16, 17]. Specifically, in the context of bone tissue engineering, it is observed that exosomes released from OBs and OCs regulate bone homeostasis by continuously transferring vital cargo like proteins, miRNAs, mRNAs etc [18, 19].

Exosomal miRNAs can be functional after getting released inside the host cells. These miRNAs can bind to the specific host cell mRNAs and thereby regulate their functionality post-transcriptionally[20]. The most common source of exosomes in bone tissue engineering applications are mesenchymal stem cells (MSCs). However, the limited source for getting MSCs makes their use difficult[21-23]. To perform deeper investigation on the importance of exosomes released by mineralizing bone cells, we conducted our study by considering mouse pre-osteoblasts MC3T3-E1 because of their well-known mineralization ability. We isolated exosomes from these cells at different stages of mineralization and checked their bone regeneration ability. The cargo analysis of the mineralized exosomes indicated that the abundantly present miRNAs are released inside the recipient cells and inhibit the expression of some of the cell cycle regulatory genes which might be involved in bone mineralization. As bone defects are local injuries and exosomes cannot be applied at those sites, the need of a solid matrix to retain exosomes and control their release was evident [24, 25]. The matrix support should be bioresorbable i.e, degrade with time until the neighbouring cells start migrating and forming mature bone tissues [26, 27] and must not incite any immunogenic reaction and this provides an advantage over metal based alloy scaffolds[21]. Due to the use of harsh chemicals during the cross-linking process of synthetic scaffolds, this creates biocompatibility issues inside the in vivo system [25, 28].

Considering the above lacunae, we synthesized a polymeric scaffold consisting of chitosan and collagen covalently cross-linked through UV polymerization. The bone regenerative potential of the DM-Exo+Scaffold were validated in critical-sized calvarial bone defect of rats. To summarize, in the present study, we unveiled that, exosomes secreted by pre-osteoblasts during their mineralization stage upon integration with a covalently cross-linked protein-polysaccharide scaffold demonstrates considerable bone healing potential of the calvarial bone defect in rats by the systematic regulation of miRNAs (Graphical representation).

2. Objectives

a. To check the mineralization potential of MC3T3-E1 cells upon treatment with DM for 7 days and 14 days.

b. To isolate, characterize the mineralized cell-derived exosomes, and checking their host cell invading ability.

c. Analysing the effect of mineralized cell derived exosomes on the unmineralized MC3T3-E1 cells upon treatment.

d. To investigate the exosomal small RNA cargo that might be involved in host cell mineralization.

e. To integrate the isolated exosomes on 3D-polymeric scaffolds for enhancing their bioavailability and checking the release rate *in vitro.*

f. Assessment of the bone regeneration ability of the exosome integrated scaffolds *in vivo.*

3. Materials and Methods

Cell culture:

Mouse pre-osteoblast cell line MC3T3-E1 (ATCC®CRL-2593™) was purchased from American Type Cell Culture Collection (ATCC) and cultured in α-minimal essential medium (HIMEDIA, α-MEM, AL221A) supplemented with 10% fetal bovine serum (FBS; In Vitro

Technologies, New York) and 1% (v/v) penicillin/streptomycin (Gibco®, Life Technologies Pty Ltd., New York). To induce osteogenic differentiation/ mineralization, the cells were cultured in DM containing 50 µg/ml L-ascorbic acid (Sigma), 100nM dexamethasone (Sigma) and 10 mM β-glycerophosphate (Sigma).

Isolation and characterization of exosomes:

Exosomes were isolated from the conditioned media of normal and mineralized cells. The normal and mineralized MC3T3-E1 conditioned media were collected, centrifuged and filtered for removal of unwanted larger particles. The filtrate was then ultracentrifuged at 1,50,000 xg for 90 min at 4°C to isolate exosomes. The dynamic light scattering and zeta potential determination for size and charge measurements were performed using a Zetasizer nanoseries instrument (Malvern, Nano ZS). For Transmission Electron Microscopy, exosomes were fixed and placed on to formavar-coated Cu TEM grids (Agar Scientific), stained with 1% uranyl acetate and air-dried. The exosomes were imaged by TEM (JEM_2100plus, JEOL, Japan) at 120 kV.

Western blotting of exosomal proteins:

Protein concentration of freshly isolated exosomes was determined using BCA Protein Assay kit (Pierce, Rockford, USA). Equal amounts of proteins (20 µg) were resolved on 8% SDS-PAGE, transferred to PVDF membrane and incubated with different primary antibodies, such as anti-CD81, anti-TSG101, anti-Calnexin, and anti-GAPDH overnight at 4-8°C. The protein expression was detected using chemiluminescent HRP substrate (ab5801) and imaged under ChemiDoc (BioRAD, Hercules, CA, USA).

Exosome uptake analysis:

The uptake of exosomes by host cells was monitored with PKH67 Green Fluorescent Cell Linker Midi Kit (Lot#MIDI67-1KT, Sigma-Aldrich, NSW, Australia) according to the manufacturer's protocols. Cells were seeded on glass coverslips and PKH67 labelled exosomes were incubated with recipient cells for 6h, 12h, and 24h. The cytoskeleton was stained with RhodamibeB-Phalloidin (Invitrogen, Thermo Fisher). Images were captured using a confocal laser scanning microscope (STELLARIS, STED, Leica) under 63 × objectives.

Cell proliferation assay and cell migration assay:

Various concentrations of exosomes (3, 10, 25, 50, and 100 µg/ml) were treated with cells and were incubated with WST-1 reagent and analysed at 440nm. For migration assay 1×105 cells were seeded on the upper compartment of a Transwell with 8 µm pore size. Exosomes along with media were added to the lower compartment. After culturing for 24h, the membranes were fixed with 4% paraformaldehyde and stained with DAPI and imaged under fluorescence microscope.

In vitro mineralization properties of MC3T3-E1 cells:

To compare the extent of mineralization of MC3T3-E1 cells treated with DM for 7 days and 14 days, ALP assay and Alizarin assay. Cells were fixed, stained, and washed and the matrix calcium deposition was checked under a brightfield microscope.

Exosomal small-RNA sequencing:

Exosomes were isolated from the cell-conditioned media of 14 days DM treated cells and the untreated confluent cells as control. The total RNA from the exosomes were isolated quantified using Qubit 4 fluorometer (Invitrogen). The small RNA library was prepared by following manufacturer's protocol (Cat. No: NGS3178, LeoNext NGS, Genes2Me). Library selection

was done with 6% non-denatured PAGE gel. The purified library product was sequenced on the Illumina NextSeq 550 platform. The raw reads were deposited in ENA (Accession No. PRJEB65457).

In silico analysis of exosomal small RNA cargo:

All the samples were sequenced with approximately 6-7 million reads. Previously published total RNA-seq data of mouse bone cell mineralization samples (GEO accession: GSE186832; SRA ID: SRP343761) were downloaded from NCBI GEO. Differential gene expression (DEGs) analysis for both miRNA and the mRNA analysis were performed using EdgeR package (v3.17). Heatmap and volcano plots were generated using Complex heatmap package and Enhance volcano plot package from R Studio.

Synthesis of chitosan and collagen cross-linked scaffolds:

Methacrylated chitosan and collagen was synthesised by reacting chitosan and collagen with methacrylic anhydride. The products were freeze-dried for 72hrs and stored at 4° C for future use. The required scaffold was fabricated by taking chitosan-methacrylate and collagen-methacrylate and UV-crosslinked.

Characterization of chitosan scaffolds:

The degree of methacrylation between chitosan (polysaccharide) and collagen (protein) was checked using proton NMR (ULTRASHIELD PLUS™ B-ACS 60 spectrometer). SEM (JEOL, Japan) was done for morphology. The rheological properties were measured using a modular compact rheometer (MCR 102 e Multi-Drive, Anton Paar). Degradation of the scaffolds was checked with 1X PBS with gentle shaking. Scaffolds were then freezed and lyophilized to get the final dry weight.

Release of exosomes from the scaffolds:

The scaffold-exo constructs were put into 1X PBS and the solvent was collected at different time points starting from 5min till 48hrs. The solvents were acquired in a flow cytometer (CytoFlex, Beckman Coulter) to check the percent positive population for PKH67. The cumulative release of exosomes was calculated.

Animal Experiments (Critical-sized calvarial defect model):

150 µg of exosomes were used for the treatment of scaffolds and cells before implantation. With the trephine bur, the critical size calvarial defect was created successfully and the combination of scaffold implantation materials was then implanted. The rats were sacrificed by CO_2 inhalation after 8 weeks of implantation. Skulls were retrieved and fixed with 10% formalin for further analysis.

Micro-CT analysis:

The rat skulls were scanned 360° with Micro-CT (SKYSCAN 1272, BRUKER) and to quantify the new bone formation, new bone volume (BV/TV) and trabecular spacing were calculated using the software.

Histological analysis:

Rat calvarial bones were decalcified using 10% EDTA (pH 7.4) for 30 days. 5 µm thin sections were prepared using microtome for histological evaluations. For Hematoxylin-eosin (H&E) staining the tissue slices were stained according to the protocol. The slides were visualized under a bright-field microscope and for analysis ImageJ software was used.

4. Results

a) To check the mineralization potential of MC3T3-E1 cells upon treatment with DM for 7 days and 14 days:

From ALP staining and ALP activity assays we found that after 7 days of DM treatment, the cells are showing significantly higher ALP deposition (Fig. 1A-i) as compared to the control where cells were grown in growth media (GM). After 14 days of treatment, the cells tend to show elevated ALP activity (Fig. 1A-ii) than that of 7day treatment. Similar results were obtained from the alizarin red staining assay, which showed an increased amount of calcium deposition with an increased time of incubation (Fig. B).
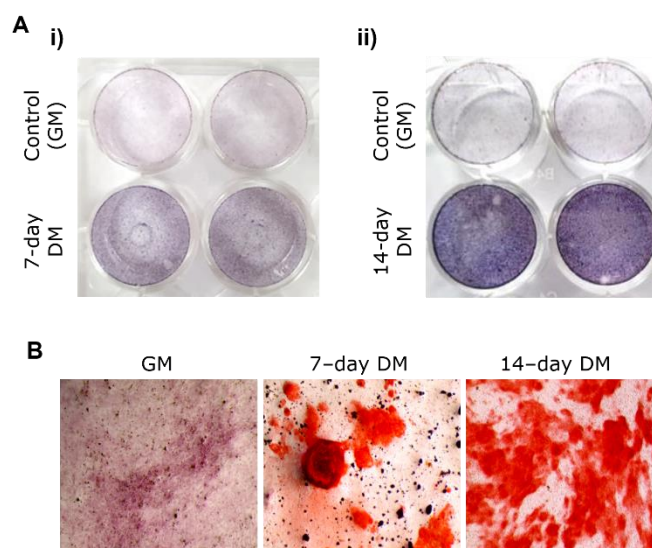

Fig. 1 (A) ALP staining after i) 7 days and ii) 14 days of differentiation upon incubation with GM and DM. (B) ARS staining of control, 7 days, and 14 days of differentiation. GM: Growth media, DM: Differentiation media.

b) To isolate, characterize the mineralized cell-derived exosomes, and checking their host cell invading ability:

Exosomes were isolated from the culture supernatants by using ultracentrifugation (Fig. 2A). The isolated vesicles were measuring about 150-200 nm in diameter (Fig. 2B), having a negative surface charge (Fig. 2C) and uniform distribution with circular morphology (Fig. 2D). The presence of EV marker proteins such as CD81 and Tsg-101 (Fig. 2F) further confirmed that the vesicles are exosomes. The PKH67 tagged exosomes were internalized by the host cells in a time dependent manner, with highest uptake at 24 h of incubation as evident from the fluorescent particles surrounding the nucleus (Fig. 2G).
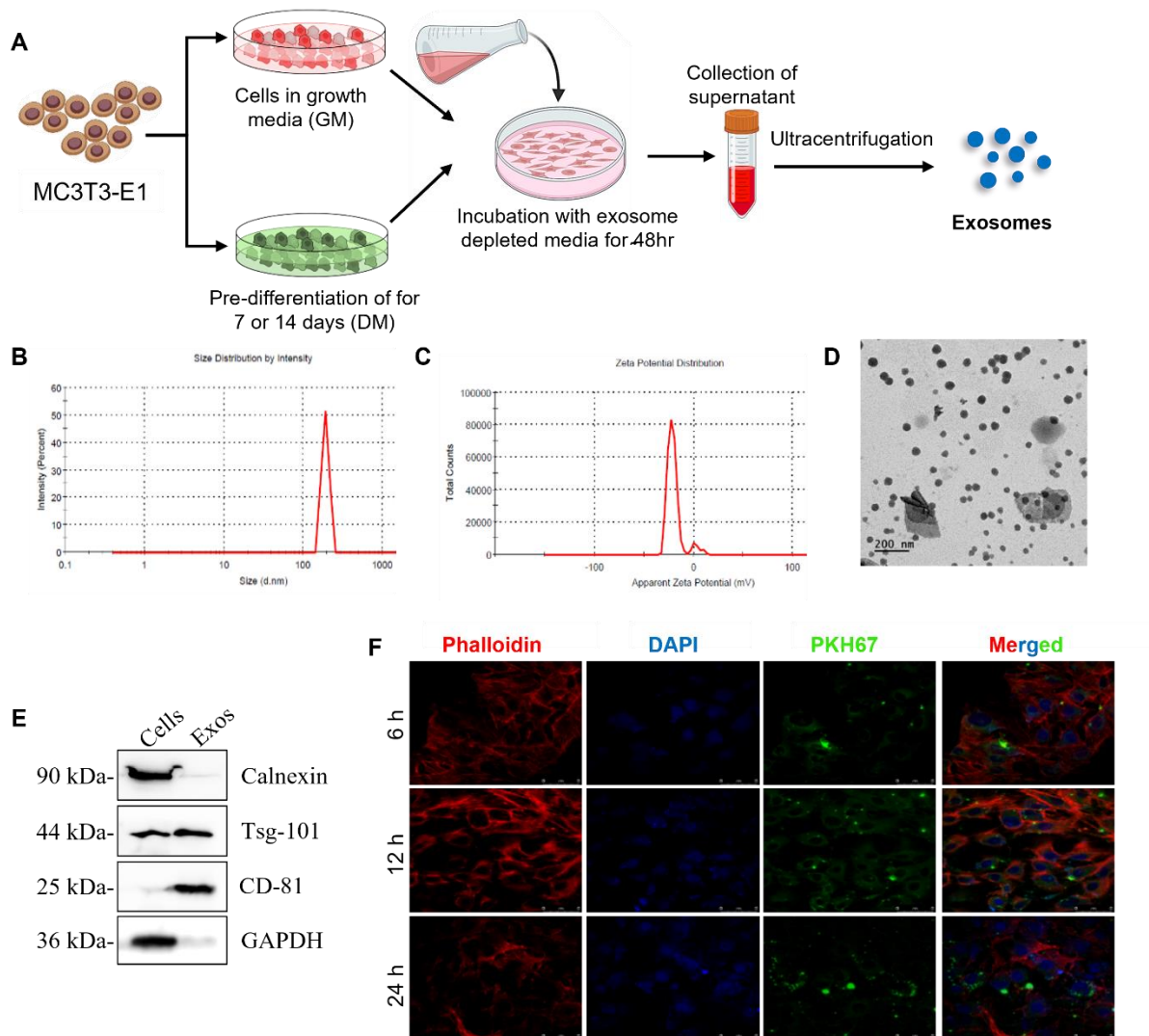
Fig. 2 (A) Schematic representation of exosome isolation from control and differentiated MC3T3-E1 cells. (B) Average size of isolated exosomes (180 nm) as depicted from DLS. (C) Negative surface charge (-20mV) detected by zeta sizer. (D) Morphology of exosomes observed by TEM. (E) Western blot analysis to show exosome markers CD81 and TSG-101. (F) Representative confocal microscopy images of PKH67 tagged exosomes (green) uptake after incubation with MC3T3-E1 cells for 6h, 12h, and 24h. Cell cytoskeleton and nuclei were stained with rhodamine-B (red) and DAPI (blue) respectively. Scale bar 25µm.

c) Analysing the effect of mineralized cell derived exosomes on the unmineralized MC3T3-E1 cells upon treatment.

For cell proliferation assay WST-1 was used by taking different concentrations of exosomes for variable time points. Results showed that exosomes can significantly promote cell proliferation with increasing concentration (Fig. 3A). The cell migration was assessed by trans-well assay. The results revealed that exosomes can also effectively promote cell migration through the membrane in a concentration dependent manner (Fig. 3B). In order to investigate the *in vitro* mineralization ability, the appropriate concentration of exosomes (50 µg/ml) from GM-cells and 7 day DM-cells were incubated with MC3T3-E1 cells for 72h. We found that the

DM-Exos were able to significantly upregulate ALP activities as compared to unmineralized cell derived exosomes (Fig. 3C).
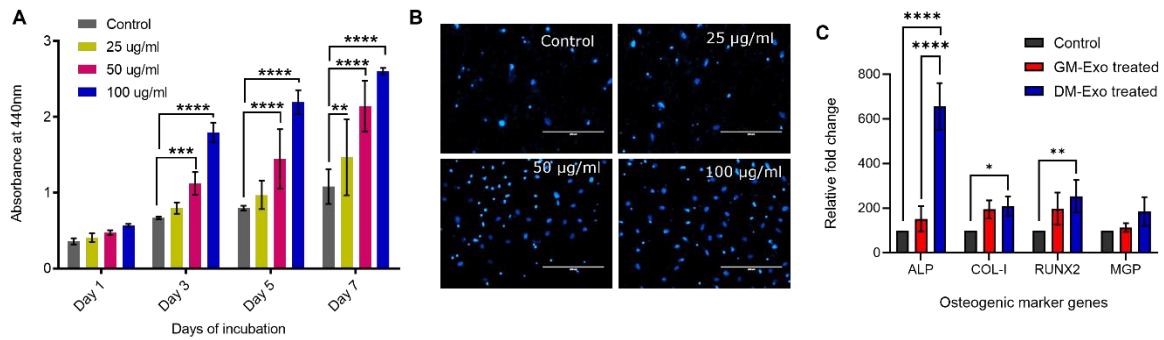

Fig. 3 (A) WST-1 assay results showing cell proliferation. (B) Trans-well image showing migration assay. (C) RT-PCR analysis of osteogenic markers (ALP, Col-1, RUNX-2 and MGP) showing increased osteogenesis with the treatment of pre-differentiated exosomes. Control was cells without any treatment.

d) To investigate the exosomal small RNA cargo that might be involved in host cell mineralization:

We identified a total of 38 differentially expressed miRNAs among which, 20 miRNAs were upregulated, while 18 miRNAs were downregulated as compared to the control group (Fig 4A). Through mRNA analysis, we pinpointed distinct sets of genes exhibiting significant upregulation (503 genes) and downregulation (277 genes) from the downloaded dataset (GSE186832)[29] (Fig 4B). The mRNA targets of the upregulated miRNAs were compared with the downregulated genes obtained from the bone cell mineralization samples within the GEO dataset. Remarkably, this comparison yielded a total of 33 genes that exhibited commonality between the two datasets, as depicted in Figure 4C.
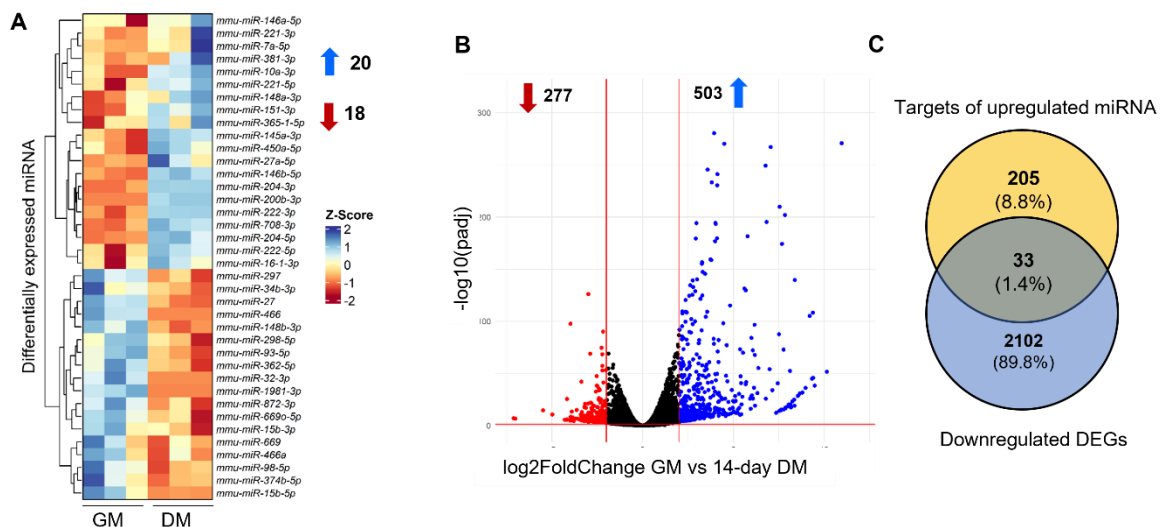

Fig. 4 (A) Heat map of the differentially expressing miRNAs in the DM treated cells as compared to the control. (B) Volcano plot for the up and downregulated genes in the dataset. (C) Comparative Venn diagram showing 33 common genes between the upregulated miRNA targets and the downregulated genes in the dataset.

e) **To integrate the isolated exosomes on 3D-polymeric scaffolds for enhancing their bioavailability and checking the release rate *in vitro*:**

A cross-linked polymeric scaffold was synthesized by using polysaccharides i.e., chitosan and collagen protein. The schematic diagram in Fig. 5A describes the mechanism of covalent cross-linking between the amino group and methyl group. Proton NMR confirmed the cross-linking between the polysaccharide and protein (Fig. 5B). The morphology of the scaffolds was observed by SEM with pore size ranging from 50 to 200nm (Fig. 5C). The rheological properties of the scaffolds are shown in Fig. 5D, which exhibited a higher G' value than G'' indicating that the elastic modulus of the scaffolds is increasing making it solid. The rate of degradation also shows faster loss of weight of scaffolds, with approximately 80% degradation within 3 days (Fig. 5E). For release profile, the exosomes were acquired in flow cytometry which suggested approximately 70-80% release after 12hr of incubation in the solvent which is co-related with the higher swelling ratio and degradation rate of the scaffolds (Fig. 5F).
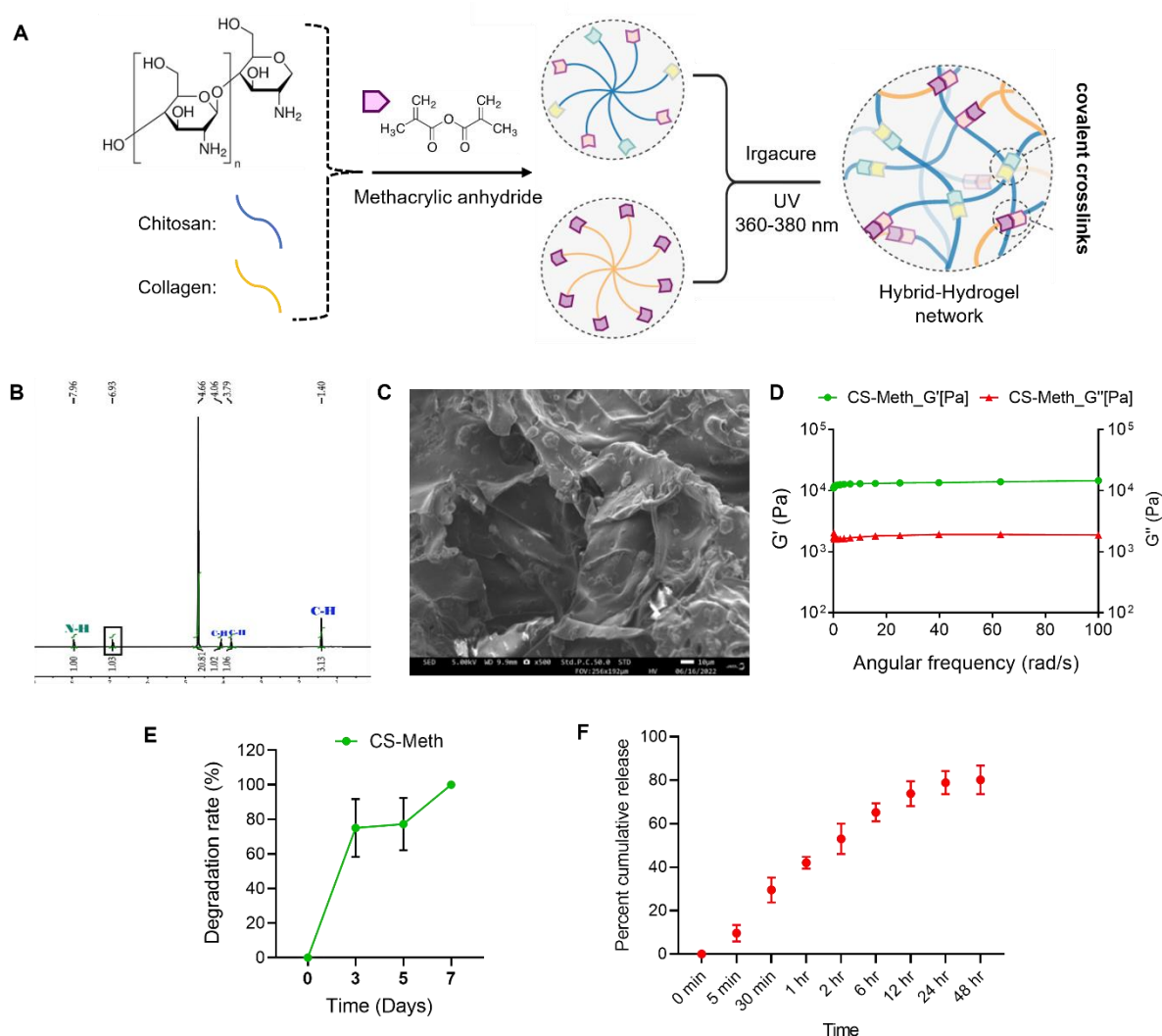

Fig. 5 (A) Covalent crosslinking of chitosan and collagen with methacrylation for hydrogel synthesis. (B) Proton NMR to ensure cross-linking. Characterization of CS-scaffolds (C) SEM image showing porous structure (50- 200nm). (D) Rheological property of scaffold. (E) Rate of scaffold degradation. (F) In vitro release profile of exosomes from scaffolds.

f) Assessment of the bone regeneration ability of the exosome integrated scaffolds *in vivo:*

After 8 weeks of implantation, the amount of new bone formation was compared to the control (with no implantation) and was evaluated by micro-CT scanning and analysis. From reconstructed micro-CT 3D images, it can be observed that very less amount of new bone was formed in the control group, while significantly higher amount of new bone formation was found in case of scaffold and scaffold exosome groups (Fig. 6A). Quantification of the microCT images in terms of new bone volume and trabecular spacing supported the above finding (Fig. 6B, C). HE staining of representative sections indicated the formation of fibrous connective tissues in the control group, while in the other three groups, solid new bone tissue formation was observed along the borders and in the centre of the defects (Fig. 6D).
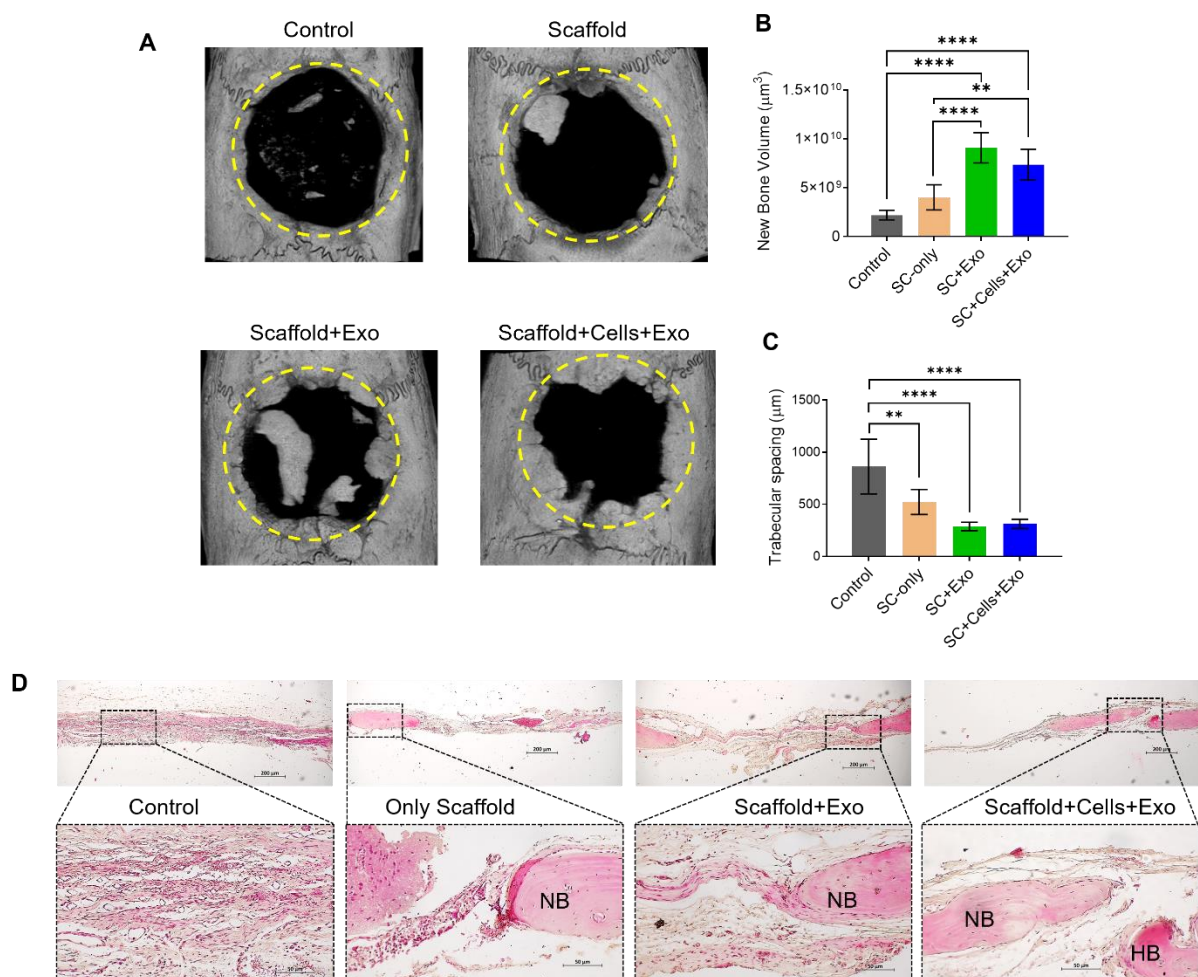

Fig. 6 (A) 3D reconstructed images of calvarial bone indicating new bone formation. Quantitative analysis of bone regeneration by (B) New bone volume and (C) Trabecular spacing. (D) HE staining. NB: New bone, HB: Host bone.

5. Statistics

GraphPad PRISM Version 8 was used for making the graphs and data analysis. One-way and two-way ANOVA with Tukey's and Sidak multiple comparison tests were used for statistics.

All data were represented as mean± standard deviation of mean (SD). P< 0.05 has been taken as a significant value. ****P<0.0001, ***P<0.0005, **P<0.005, *P<0.05.

6. Discussion

Osteoblasts are known to potentially regulate bone remodelling at the mineralization stage [30, 21, 31]. However, the role of the different stages of mineralization upon the regeneration process remains largely unknown. Our study shows that pre-mineralization of mouse bone cells (MC3T3-E1) for 7 and 14 days can enhance their differentiation potential and the exosomes released from them can enter into the undifferentiated recipient cells to promote their differentiation. We also observe that exosomes secreted from osteoblast cells in their later stage of differentiation, accelerate the process in the recipient cells more prominently.

In this study, exosomes were isolated from the mouse pre-osteoblasts (MC3T3-E1) after induction with DM for 7 days and 14 days. We found that the cells showed enhanced mineralization activities in terms of ALP and alizarin staining after 7 days of treatment compared to the control (Fig 1). The PKH67 labelled exosomes endocytosed into the host cells in a time dependent manner (Fig 2F). The amounts of exosomes had a directly proportional effect on the cell proliferation and migration of cells (Fig 3A, B), which is in line with previously reported findings[32, 33]. The exosome treated cells displayed enhanced osteogenicity and the expression was higher with DM treatment than GM treatment (Fig 3C). It is reported that exosomes from pre-mineralized MSCs or ADSCs have better host cell differentiating capacity than exosomes from normal stem cell derived exosomes[21]. In line with these studies, our findings indicated that the exosomes secreted during the process of mineralization contain essential factors to positively regulate the bone regeneration process[21, 30].

To explore the essential factors, present within the mineralized exosomes, we performed small RNA sequencing which revealed the differentially regulated miRNAs in the exosomes of 14 day DM-treated cells compared to the exosomes from control cells. Comparison of the upregulated mRNAs targets with the downregulated genes of the cells, we found 33 common genes, involved mostly in cell cycle progression and transcription regulation (Fig 4C). We propose that suppression of these genes by exosomal miRNAs might be enhancing the bone mineralization potential of the host cells (pre-osteoblasts) after 72hrs of treatment.

The major challenge of using exosomes for critical sized bone defects is to retain them at the site of bone defect. For localized delivery of exosomes at the defect site, a matrix is essential to hold them. As synthetic matrix or graft materials, bioactive ceramics[34], titanium scaffolds[21], 3D scaffolds fabricated from poly(L-lactic acid) (PLLA)[35] have been previously used to fill the gap created by bone defects. Exosomes are used as bioactive molecules to enhance the performance of these graft materials. We demonstrated that the matrix composed of chitosan and collagen provides a suitable matrix for exosome integration and release. Most of the exosomes were able to get released before the scaffold completely gets degraded, thus providing the necessary structural support to the exosomes. The calvarial defect of 8 mm shows bone regeneration by the scaffold laden with exosomes within 8 weeks of implantation. The microCT reveals the formation of new bone with proper trabecular spacing (Fig 6) and H & E staining confirms mature collagen formation at the defect site.

7. Impact of the research in the advancement of knowledge or benefit to mankind
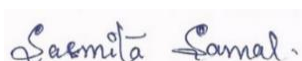
The current study clearly advances the existing knowledge on the following aspects; 1) normal osteoblasts can release exosomes upon treatment with DM for 7 days notably different from what has been reported with exosomes from stem cells, 2) the polysaccharide-protein matrix provides the required bioresorbable support, promoting ECM formation unlike their metal counterparts with sustained release of exosomes. The ECM promoting scaffolds loaded with mineralized exosomes present a cell free approach to regenerate bone by overcoming notable lacunae in the field. This platform can facilitate the local activity of exosomes when preserved in appropriate storage conditions, which keeps intact the favourable properties of exosomes, without off-target effects. Our results provide strong evidence to suggest that exosomes derived from mineralizing pre-osteoblasts together with an ECM promoting matrix provide pro-mineralization cues to drive cells at the local defect site towards osteogenic differentiation.

8. Literature references

(1) Bonafede, M.; Espindle, D.; Bower, A. G. The direct and indirect costs of long bone fractures in a working age US population. *J Med Econ* **2013**, *16* (1), 169-178. DOI: 10.3111/13696998.2012.737391 From NLM.

(2) Delea, T.; Langer, C.; McKiernan, J.; Liss, M.; Edelsberg, J.; Brandman, J.; Sung, J.; Raut, M.; Oster, G. The Cost of Treatment of Skeletal-Related Events in Patients with Bone Metastases from Lung Cancer. *Oncology* **2004**, *67* (5-6), 390-396. DOI: 10.1159/000082923.

(3) Dimitriou, R.; Jones, E.; McGonagle, D.; Giannoudis, P. V. Bone regeneration: current concepts and future directions. *BMC Medicine* **2011**, *9* (1), 66. DOI: 10.1186/1741-7015-9-66.

(4) Loeffler, J.; Duda, G. N.; Sass, F. A.; Dienelt, A. The Metabolic Microenvironment Steers Bone Tissue Regeneration. *Trends in Endocrinology & Metabolism* **2018**, *29* (2), 99-110. DOI: https://doi.org/10.1016/j.tem.2017.11.008.

(5) Bosch, C.; Melsen, B.; Vargervik, K. Importance of the Critical-Size Bone Defect in Testing Bone-Regenerating Materials. *Journal of Craniofacial Surgery* **1998**, *9* (4), 310-316.

(6) Roddy, E.; DeBaun, M. R.; Daoud-Gray, A.; Yang, Y. P.; Gardner, M. J. Treatment of critical-sized bone defects: clinical and tissue engineering perspectives. *European Journal of Orthopaedic Surgery & Traumatology* **2018**, *28* (3), 351-362. DOI: 10.1007/s00590-017-2063-0.

(7) Wildemann, B.; Ignatius, A.; Leung, F.; Taitsman, L. A.; Smith, R. M.; Pesántez, R.; Stoddart, M. J.; Richards, R. G.; Jupiter, J. B. Non-union bone fractures. *Nature Reviews Disease Primers* **2021**, *7* (1), 57. DOI: 10.1038/s41572-021-00289-8.

(8) Quarto, R.; Mastrogiacomo, M.; Cancedda, R.; Kutepov, S. M.; Mukhachev, V.; Lavroukov, A.; Kon, E.; Marcacci, M. Repair of Large Bone Defects with the Use of Autologous Bone Marrow Stromal Cells. *New England Journal of Medicine* **2001**, *344* (5), 385-386. DOI: 10.1056/nejm200102013440516.

(9) Calori, G. M.; Mazza, E.; Colombo, M.; Ripamonti, C. The use of bone-graft substitutes in large bone defects: Any specific needs? *Injury* **2011**, *42*, S56-S63. DOI: https://doi.org/10.1016/j.injury.2011.06.011.

(10) Stem Cells: Promises Versus Limitations. *Tissue Engineering Part B: Reviews* **2008**, *14* (1), 53-60. DOI: 10.1089/teb.2007.0216.

(11) Rong, Z.; Wang, M.; Hu, Z.; Stradner, M.; Zhu, S.; Kong, H.; Yi, H.; Goldrath, A.; Yang, Y.-G.; Xu, Y.; et al. An Effective Approach to Prevent Immune Rejection of Human ESC-Derived Allografts. *Cell Stem Cell* **2014**, *14* (1), 121-130. DOI: https://doi.org/10.1016/j.stem.2013.11.014.

(12) Immunogenicity of Adult Mesenchymal Stem Cells: Lessons from the Fetal Allograft. *Stem Cells and Development* **2005**, *14* (3), 252-265. DOI: 10.1089/scd.2005.14.252.

(13) Diederichs, S.; Shine, K. M.; Tuan, R. S. The promise and challenges of stem cell-based therapies for skeletal diseases. *BioEssays* **2013**, *35* (3), 220-230. DOI: https://doi.org/10.1002/bies.201200068.

(14) Bobrie, A.; Colombo, M.; Raposo, G.; Théry, C. Exosome Secretion: Molecular Mechanisms and Roles in Immune Responses. *Traffic* **2011**, *12* (12), 1659-1668. DOI: https://doi.org/10.1111/j.1600-0854.2011.01225.x.

(15) Kowal, J.; Tkach, M.; Théry, C. Biogenesis and secretion of exosomes. *Current Opinion in Cell Biology* **2014**, *29*, 116-125. DOI: https://doi.org/10.1016/j.ceb.2014.05.004.

(16) Keerthikumar, S.; Chisanga, D.; Ariyaratne, D.; Al Saffar, H.; Anand, S.; Zhao, K.; Samuel, M.; Pathan, M.; Jois, M.; Chilamkurti, N.; et al. ExoCarta: A Web-Based Compendium of Exosomal Cargo. *Journal of Molecular Biology* **2016**, *428* (4), 688-692. DOI: https://doi.org/10.1016/j.jmb.2015.09.019.

(17) Pathan, M.; Fonseka, P.; Chitti, S. V.; Kang, T.; Sanwlani, R.; Van Deun, J.; Hendrix, A.; Mathivanan, S. Vesiclepedia 2019: a compendium of RNA, proteins, lipids and metabolites in extracellular vesicles. *Nucleic Acids Research* **2018**, *47* (D1), D516-D519. DOI: 10.1093/nar/gky1029 (acccessed 3/10/2023).

(18) Gao, M.; Gao, W.; Papadimitriou, J. M.; Zhang, C.; Gao, J.; Zheng, M. Exosomes—the enigmatic regulators of bone homeostasis. *Bone Research* **2018**, *6* (1), 36. DOI: 10.1038/s41413-018-0039-2.

(19) Samal, S.; Dash, P.; Dash, M. Drug Delivery to the Bone Microenvironment Mediated by Exosomes: An Axiom or Enigma. *Int J Nanomedicine* **2021**, *16*, 3509-3540. DOI: 10.2147/ijn.S307843 From NLM.

(20) Valadi, H.; Ekström, K.; Bossios, A.; Sjöstrand, M.; Lee, J. J.; Lötvall, J. O. Exosome-mediated transfer of mRNAs and microRNAs is a novel mechanism of genetic exchange between cells. *Nature Cell Biology* **2007**, *9* (6), 654-659. DOI: 10.1038/ncb1596.

(21) Zhai, M.; Zhu, Y.; Yang, M.; Mao, C. Human Mesenchymal Stem Cell Derived Exosomes Enhance Cell-Free Bone Regeneration by Altering Their miRNAs Profiles. *Advanced Science* **2020**, *7* (19), 2001334. DOI: https://doi.org/10.1002/advs.202001334.

(22) Rani, S.; Ryan, A. E.; Griffin, M. D.; Ritter, T. Mesenchymal Stem Cell-derived Extracellular Vesicles: Toward Cell-free Therapeutic Applications. *Molecular Therapy* **2015**, *23* (5), 812-823. DOI: https://doi.org/10.1038/mt.2015.44.

(23) Li, W.; Liu, Y.; Zhang, P.; Tang, Y.; Zhou, M.; Jiang, W.; Zhang, X.; Wu, G.; Zhou, Y. Tissue-Engineered Bone Immobilized with Human Adipose Stem Cells-Derived Exosomes Promotes Bone Regeneration. *ACS Applied Materials & Interfaces* **2018**, *10* (6), 5240-5254. DOI: 10.1021/acsami.7b17620.

(24) Liu, X.; Ma, P. X. Polymeric Scaffolds for Bone Tissue Engineering. *Annals of Biomedical Engineering* **2004**, *32* (3), 477-486. DOI: 10.1023/B:ABME.0000017544.36001.8e.

(25) Roseti, L.; Parisi, V.; Petretta, M.; Cavallo, C.; Desando, G.; Bartolotti, I.; Grigolo, B. Scaffolds for Bone Tissue Engineering: State of the art and new perspectives. *Materials Science and Engineering: C* **2017**, *78*, 1246-1262. DOI: https://doi.org/10.1016/j.msec.2017.05.017.

(26) Yan, J.; Miao, Y.; Tan, H.; Zhou, T.; Ling, Z.; Chen, Y.; Xing, X.; Hu, X. Injectable alginate/hydroxyapatite gel scaffold combined with gelatin microspheres for drug delivery and bone tissue engineering. *Materials Science and Engineering: C* **2016**, *63*, 274-284. DOI: https://doi.org/10.1016/j.msec.2016.02.071.

(27) Wei, G.; Ma, P. X. Structure and properties of nano-hydroxyapatite/polymer composite scaffolds for bone tissue engineering. *Biomaterials* **2004**, *25* (19), 4749-4757. DOI: https://doi.org/10.1016/j.biomaterials.2003.12.005.

(28) Qu, H.; Fu, H.; Han, Z.; Sun, Y. Biomaterials for bone tissue engineering scaffolds: a review. *RSC Advances* **2019**, *9* (45), 26252-26262, 10.1039/C9RA05214C. DOI: 10.1039/C9RA05214C.

(29) Rummukainen, P.; Tarkkonen, K.; Dudakovic, A.; Al-Majidi, R.; Nieminen-Pihala, V.; Valensisi, C.; Hawkins, R. D.; van Wijnen, A. J.; Kiviranta, R. Lysine-Specific Demethylase 1 (LSD1) epigenetically controls osteoblast differentiation. *PLOS ONE* **2022**, *17* (3), e0265027. DOI: 10.1371/journal.pone.0265027.

(30) Cui, Y.; Luan, J.; Li, H.; Zhou, X.; Han, J. Exosomes derived from mineralizing osteoblasts promote ST2 cell osteogenic differentiation by alteration of microRNA expression. *FEBS Letters* **2016**, *590* (1), 185-192. DOI: https://doi.org/10.1002/1873-3468.12024.

(31) Takeuchi, R.; Katagiri, W.; Endo, S.; Kobayashi, T. Exosomes from conditioned media of bone marrow-derived mesenchymal stem cells promote bone regeneration by enhancing angiogenesis. *PLOS ONE* **2019**, *14* (11), e0225472. DOI: 10.1371/journal.pone.0225472.

(32) Jia, L.; Zhou, X.; Huang, X.; Xu, X.; Jia, Y.; Wu, Y.; Yao, J.; Wu, Y.; Wang, K. Maternal and umbilical cord serum-derived exosomes enhance endothelial cell proliferation and migration. *The FASEB Journal* **2018**, *32* (8), 4534-4543. DOI: https://doi.org/10.1096/fj.201701337RR.

(33) Choi, E. W.; Seo, M. K.; Woo, E. Y.; Kim, S. H.; Park, E. J.; Kim, S. Exosomes from human adipose-derived stem cells promote proliferation and migration of skin fibroblasts. *Experimental Dermatology* **2018**, *27* (10), 1170-1172. DOI: https://doi.org/10.1111/exd.13451.

(34) Teotia, A. K.; Qayoom, I.; Singh, P.; Mishra, A.; Jaiman, D.; Seppälä, J.; Lidgren, L.; Kumar, A. Exosome-Functionalized Ceramic Bone Substitute Promotes Critical-Sized Bone Defect Repair in Rats. *ACS Applied Bio Materials* **2021**, *4* (4), 3716-3726. DOI: 10.1021/acsabm.1c00311.

(35) Swanson, W. B.; Zhang, Z.; Xiu, K.; Gong, T.; Eberle, M.; Wang, Z.; Ma, P. X. Scaffolds with controlled release of pro-mineralization exosomes to promote craniofacial bone healing without cell transplantation. *Acta Biomaterialia* **2020**, *118*, 215-232. DOI: https://doi.org/10.1016/j.actbio.2020.09.052.

Applicant

Sasmita Samal

5th Year Ph.D. student,

Institute of Life Sciences,

Bhubaneswar